



DRUG DEVELOPMENT AND INDUSTRIAL PHARMACY  
Vol. 28, No. 10, pp. 1213–1220, 2002

RESEARCH PAPER

## Spherical Crystallization of Celecoxib

A. R. Paradkar,\* A. P. Pawar, J. K. Chordiya,  
V. B. Patil, and A. R. Ketkar

*Department of Pharmaceutics, Bharati Vidyapeeth  
Deemed University, Poona College of Pharmacy,  
Erandwane, Pune 411 038, Maharashtra, India*

### ABSTRACT

*Celecoxib exhibits poor flow properties and compressibility. Spherical crystallization of celecoxib was carried out using the solvent change method. An acetone:dichloromethane (DCM):water system was used where DCM acted as a bridging liquid and acetone and water as good and bad solvent, respectively. Hydroxypropylmethylcellulose (HPMC) was used to impart strength and sphericity to the agglomerates. The effect of amount of bridging liquid and speed of agitation was studied using  $3^2$  factorial design. Primary properties of the agglomerates were evaluated by infrared spectroscopy, powder X-ray diffraction, and differential scanning calorimetry. The effect of variables on micromeritic, mechanical, compressional, and dissolution behavior was evaluated by response surface methodology. Particle size, bulk density, mean yield pressure (MYP), and drug release were found to be significantly affected by either of the two variables. Interaction of variables significantly affected the MYP.*

**Key Words:** *Spherical crystallization; Celecoxib; Factorial design; Response surface methodology; Tableting properties*

### INTRODUCTION

Spherical crystallization is a particle design technique, which involves crystallization and simulta-

neous agglomeration of drug in the presence of bridging liquid. Spherical crystallization has been applied as a particle size enlargement technique for many drugs.<sup>[1–3]</sup> Apart from particle enlarge-

\*Corresponding author. Fax: +91-20-543 9383; E-mail: arparadkar@rediffmail.com

ment,<sup>[4,5]</sup> it has also been applied for various purposes such as taste-masking, e.g., enoxacin,<sup>[6]</sup> crystallinity and crystal form changes, e.g., tolbutamide<sup>[7–10]</sup> and tranilast anhydrate.<sup>[11]</sup>

Celecoxib is the first selective COX-2 inhibitor that exhibits clinically meaningful 375-fold selectivity for COX-2 over COX-1. It has been approved for use in indications of osteoarthritis and rheumatoid arthritis in a dosage regimen of 200–400 mg daily. Preformulation study of celecoxib shows that it has long needle-shaped crystals with poor flow properties and compressibility. Presently it is available in capsules. The purpose of the present work is to improve the micromeritic and compressional properties of celecoxib by a spherical crystallization process. Response surface methodology was used as an effective technique to analyze the effect of variables on the dependent variables.

## MATERIALS

Celecoxib was obtained as a gift sample from Emcure Pharmaceuticals Ltd., Pune, India. Hydroxypropylmethylcellulose (HPMC, 50 cps) was purchased from Research Lab., Mumbai, India. Acetone, dichloromethane (DCM), and all other chemicals were of analytical grade.

## METHODS

### Spherical Crystallization

A solution of celecoxib (3 g) in 6 mL acetone was added to a solution of HPMC (210 mg) in DCM. Drug was crystallized by adding the drug solution to a 500 mL capacity, wall-baffled vessel containing 100 mL distilled water. The mixture was stirred continuously using a controlled speed stirrer (Eurostar, IKA Labortechnik, Staufen, Germany) to obtain spherical agglomerates. The agglomerates were separated by filtration and dried at room temperature. The amount of DCM and speed of agitation were selected as independent variables. Experiments were carried out as per 3<sup>2</sup> factorial design. Coded and actual values of variables and the experimental design are given in Table 1.

**Table 1**

*Experimental Design with Coded Levels and Actual Values of Variables*

Batch	Variable X1: Amount of DCM (mL)	Variable X2: Speed of Agitation (rpm)
C1	4 (–1) <sup>a</sup>	600 (–1)
C2	8 (1)	600 (–1)
C3	4 (–1)	800 (1)
C4	6 (0)	600 (–1)
C5	8 (1)	800 (1)
C6	6 (0)	800 (1)
C7	4 (–1)	700 (0)
C8	8 (1)	700 (0)
C9	6 (0)	700 (0)

<sup>a</sup>Values in parentheses indicate coded levels.

### Evaluation of Agglomerates

#### Drug Content

Agglomerates (50 mg) were triturated and dissolved in 250 mL 0.1 N NaOH by sonicating for 30 min. The solution was filtered and after sufficient dilution with 0.1 N NaOH analyzed spectrophotometrically at 251.2 nm (JASCO-V500). Drug content was calculated from the calibration curve of celecoxib in 0.1 N NaOH.

#### Surface Topography

The photomicrographs (magnification 62.5×) of agglomerates were taken on a trinocular optical stereomicroscope (Zeiss, Gottingen, Germany). The tracings obtained from photomicrographs were used to calculate the circulatory factor ( $S$ )<sup>[12]</sup> as:

$$S = P^2 / (12.56 \times A)$$

where  $A$  is area (cm<sup>2</sup>) and  $P$  is perimeter (cm).

#### Infrared Spectroscopy

The infrared spectra of celecoxib and agglomerates were recorded on a JASCO-FTIR 5300 by the KBr pellet technique. The pellets were prepared on a KBr-press (Spectralab, Mumbai, India).

#### Differential Scanning Calorimetry

Thermograms were obtained using a DSC Mettler Toledo 821°. Accurately weighed samples of

celecoxib and agglomerates of batch C9 were hermetically sealed in an aluminum crucible. The system was purged with nitrogen gas at a flow rate of 100 mL/min to maintain an inert atmosphere. Heating was done from 25 to 300°C at a rate of 10°C/min.

#### Powder X-ray Diffraction

Powder X-ray diffraction patterns of the pure celecoxib and agglomerates of batch C9 were obtained (X-ray diffractometer, Philips), using Cu K $\alpha$  radiation ( $\lambda = 1.542 \text{ \AA}$ ) at 30 kV voltage and current of 30 mA. The data was recorded over a range of 2° to 50° at a scanning rate of  $1 \times 10^4 \text{ C/sec}$ , using a chart speed of 5 mm/2°.

#### Micromeritic Properties

Particle size distribution was studied by sieve analysis technique. Flowability of the agglomerates was assessed by determining the angle of repose by a fixed funnel method.<sup>[13]</sup> Bulk density was determined using bulk density test apparatus (Electrolab, Mumbai, India).

#### Mechanical Properties

Crushing strength of agglomerates was determined using Jarosz and Parrot's mercury load cell method.<sup>[14]</sup> It was carried out using a 10-mL glass hypodermic syringe. The modifications include removal of the tip of the syringe and the top end of the plunger. The barrel was used as a hollow support and guide tube with close fitting to the plunger. A window was cut at the lower end of the barrel to facilitate placement of the agglomerate on the base platen. The plunger acted as a movable platen. It was set directly on the agglomerate, positioned on the lower platen. Mercury was added to the plunger at a rate of 10 g/sec from a separating funnel, from a fixed height. The total weight of mercury plus that of plunger required to break the agglomerate was the crushing strength.

For determination of tensile strength, 600 mg agglomerates were compressed using a hydraulic press (Spectralab, Mumbai, India) at 0.5 tons for 1 min. The compacts were stored in a desiccator for 24 hr to allow elastic recovery. The thickness and diameter were measured for each compact. The hardness of each compact was then measured using a Monsanto tablet hardness tester. The tensile

strength  $\sigma_t$  of the compact ( $\text{kg/cm}^2$ ) was calculated using the following equation:<sup>[15]</sup>

$$\sigma_t = 2F/\pi Dt$$

where  $F$ ,  $D$ , and  $t$  are hardness (kg), compact diameter (cm), and thickness (cm), respectively.

#### Compressional Properties

Celecoxib powder and agglomerates ( $600 \pm 5 \text{ mg}$ ) were compressed at compaction pressure of 0.5, 1, 1.5, 2, 2.5, and 3 tons for 1 min using a hydraulic press. The compacts of zero porosity were obtained by compressing the agglomerates at 7 tons.<sup>[16]</sup> The results were put into a Heckel equation to obtain the mean yield pressure (MYP):

$$\ln(1/1 - D) = KP + A$$

where  $P$  is compaction pressure (tons),  $D$  is packing fraction, and  $K$  and  $A$  are constants. The mean yield pressure is the reciprocal of  $K$ .

#### In Vitro Dissolution

The dissolution was carried out in USP dissolution test apparatus (DA-6, Veego Scientific, Mumbai, India). The dissolution medium used was 900 mL of 0.1 N NaOH. The agglomerates were weighed according to the drug content of respective batches and their compacts were prepared at 0.5 tons for a dwell time of 1 min; 5% of sodium starch glycolate was added as a disintegrant. The medium was stirred at 100 rpm using paddles at  $37 \pm 2^\circ \text{C}$ . Samples were collected and analyzed spectrophotometrically at 251.2 nm. Dissolution of marketed celecoxib capsules (Revibra®, Dr. Reddy's Laboratories, Hyderabad, India) was also carried out.

## RESULTS AND DISCUSSION

Spherical agglomerates of celecoxib were obtained by the solvent change method. A typical spherical crystallization system involves a good solvent, a bad solvent, and a bridging liquid. The selection of these solvents depends on the miscibility of the solvents and the solubility of drug in individual solvents. Taking into consideration the poor solubility of celecoxib along with mutual solvent miscibility and polarity, acetone ( $\delta = 9.8$ ), DCM ( $\delta = 9.9$ ), and water ( $\delta = 23.4$ )<sup>[17,18]</sup> were selected as good solvent, bridging liquid, and bad solvent, respectively. Hydroxypropylmethylcellulose was added to the system to impart strength and spheric-

ity to the agglomerates. Morishima et al.<sup>[19]</sup> observed that the presence of HPMC on the particle surface increases particle–particle interaction, causing faster squeezing out of DCM to the surface, resulting in increased particle size.

The yield obtained for various batches as per factorial design was in the range of 85–97%, with the drug content in the range of 90–94%.

### Evaluation of Agglomerates

#### Surface Topography

The celecoxib crystals were fine needles. The agglomerates obtained (Fig. 1) were spheres with circularity factor ranging between 1 and 1.09. Both

the amount of DCM and the speed of agitation were found to affect the size and surface smoothness of agglomerates. At higher levels of speed of agitation, smaller and denser compacts with smooth surface were obtained due to higher breaking force and faster solvent evaporation, and in turn agglomerate compaction. Larger droplet size and longer time for formation of agglomerates led to less dense agglomerates with rough surface, at higher levels of DCM. Agglomerates obtained at lower levels of both the variables were smaller with irregular surface.

#### Crystal Characterization

Infrared spectra of celecoxib and agglomerate showed characteristic peaks of drug at  $3342\text{ cm}^{-1}$

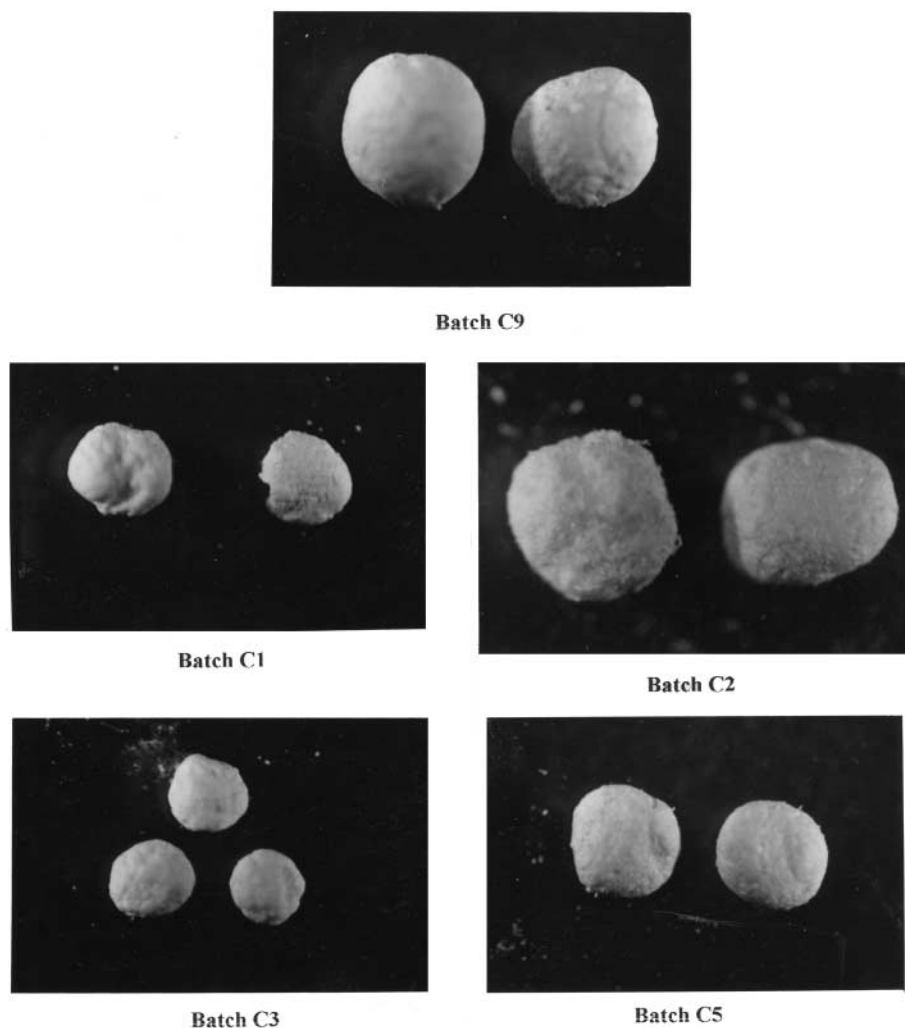


**Figure 1.** Photomicrographs of celecoxib agglomerates at  $62.5\times$  magnification.

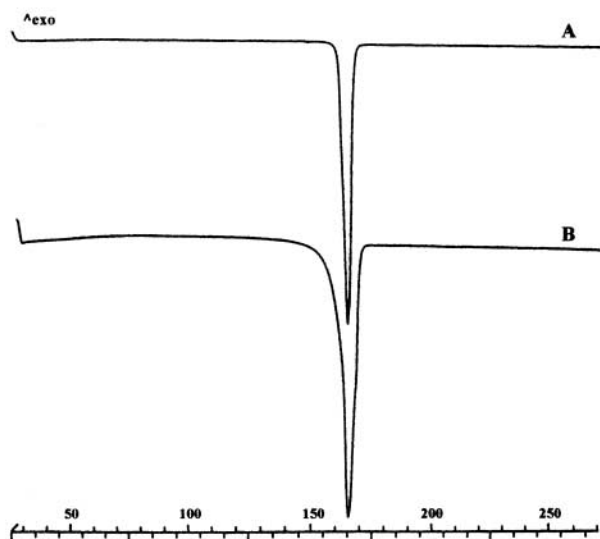


**Figure 2.** DSC thermograms of celecoxib (A) and batch C9 (B).

(NH str., primary amine),  $1165\text{ cm}^{-1}$  and  $1348\text{ cm}^{-1}$  (S=O asymmetric and symmetric str., respectively), and  $1275\text{ cm}^{-1}$  and  $1230\text{ cm}^{-1}$  ( $-\text{CF}_3$ ). Differential scanning calorimetry thermograms of celecoxib and the agglomerate showed a sharp melting endotherm (Fig. 2). The celecoxib crystals melted at  $163.3^\circ\text{C}$  with enthalpy of  $-91.71\text{ J/g}$ . The melting endotherm for drug in agglomerate occurred at  $161.2^\circ\text{C}$  with decreased enthalpy of  $-79.81\text{ J/g}$ , indicating decreased crystallinity. Powder x-ray diffraction spectra of celecoxib and agglomerate indicate significant decrease in crystallinity, as shown in Fig. 3.

#### Factorial Design

The data obtained from various batches as per factorial design was fitted using the model:

$$Y = \beta_0 + \beta_1 X_1 + \beta_2 X_2 + \beta_{12} X_1 X_2 + \beta_{11} X_1 X_1 + \beta_{22} X_2 X_2 \quad (1)$$

The data analysis was carried out using multiple regression analysis and analysis of variance (ANOVA) using UNISTAT<sup>®</sup> version 3, Megalon, USA. The results of regression analysis are shown in Table 2.

#### Micromeritic Properties

Sieve analysis data was found to follow the Rosin–Rammler distribution.<sup>[20]</sup> The average particle size was determined using the following equation:

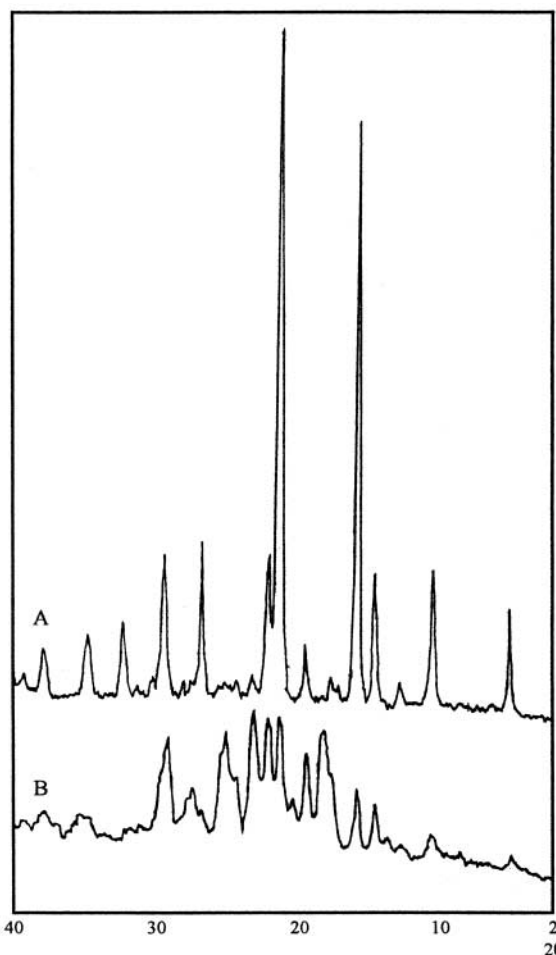


**Figure 3.** Powder x-ray diffraction spectra of celecoxib (A) and batch C9 (B).

$$\log(-\log R/100) = n \log d + \log b + \log(\log e) \quad (2)$$

where  $d$ ,  $R$ , and  $b$  denote Rosin–Rammler diameter (RRD), cumulative residual per cent by weight, and constant, respectively.

Average RRD was found to be  $810\mu\text{m}$  and exhibited a curvilinear relationship with speed of agitation. As shown in Fig. 4, after a critical speed, the size of the agglomerates decreases significantly with increase in the speed of agitation. The amount of DCM did not show any significant effect on RRD.

The average bulk density of the agglomerates was found to be  $0.22\text{ g/cc}$ . It was a function of the amount of DCM with a negative coefficient and exhibited a curvilinear relationship (Fig. 5).

**Table 2**

Summary of Regression Results for the Measured Responses

Coefficients	MYP ( $P_y$ )	Bulk Density	Angle of Repose	RRD	Tensile Strength	$D_{45}$
$\beta_0$	1.55	0.22	32.66	809.74	10.29	95.96
$\beta_1$	-0.237	-0.033	1.621	—	-1.549	-1.73
$\beta_2$	—	—	—	-115.68	—	0.74
$\beta_1\beta_2$	0.456	—	—	—	—	—
$\beta_1\beta_1$	—	-0.035	—	—	—	2.32
$\beta_2\beta_2$	-0.558	—	-2.588	-50.618	—	-2.33
$R^2$	0.83	0.927	0.607	0.998	0.435	0.81
$P$	0.0222	0.0004	0.000	0.0001	0.0002	0.0003

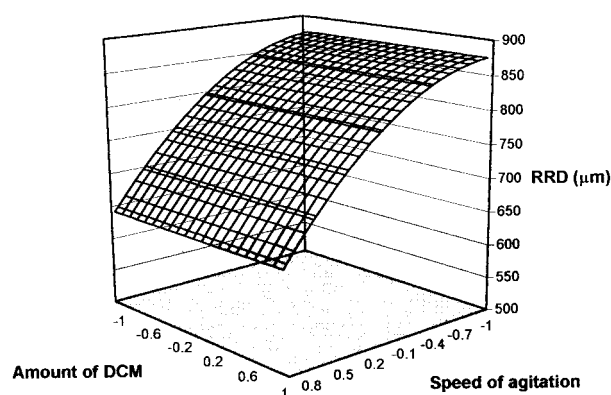


**Figure 4.** Effect of variables on Rosin–Rammler Diameter (RRD).

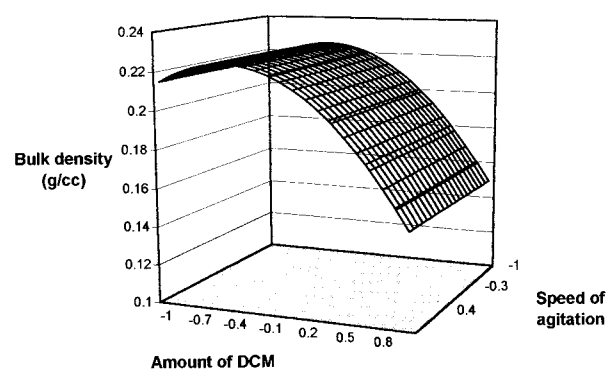


**Figure 5.** Effect of variables on bulk density.

The angle of repose was in the range of 28° to 34° and independent of the variables.

### Mechanical Properties

The crushing strength of the agglomerates was in the range of 13–29 g and was unaffected by the

variables. The agglomerates of batch C4 exhibited the highest crushing strength. The tensile strength of agglomerates compacted at 0.5 tons was in the range of 7.3–13.5 kg/cm<sup>2</sup>. The tensile strength decreases linearly with increase in volume of DCM during preparation of agglomerates. This may be attributed to loss of HPMC during the spherical crystallization process due to longer periods of agitation and lower viscosity of the droplet. But this variable accounts for only 43% of the variation in tensile strength.

### Compressional Properties

The mean yield pressure ( $P_y$ ) value of celecoxib crystals was found to be 2.5 tons, indicating poor compressibility. The MYP values for agglomerates were in the range of 0.5–1.9 tons. The regression analysis data shows that 83% of the variation in MYP is a linear function of the volume of DCM, and has a quadratic relation with speed of agitation. The interaction coefficient was also found to be significant.

The response surface for MYP (Fig. 6) shows that at lower levels of DCM, MYP increases with increase in speed of agitation, which may be due to interaction between the variables. Faster evaporation of bridging liquid at higher agitation speed does not allow higher densification during formation of the agglomerate. At higher levels of DCM, MYP increases with increase in speed of agitation due to the compactness imparted to the agglomerates. At lower speed of agitation the effect of DCM predominates, where with increase in DCM, MYP decreases due to increase in loss of HPMC. This effect diminishes with increase in speed of agitation. At lower agitation speed and high amount of DCM

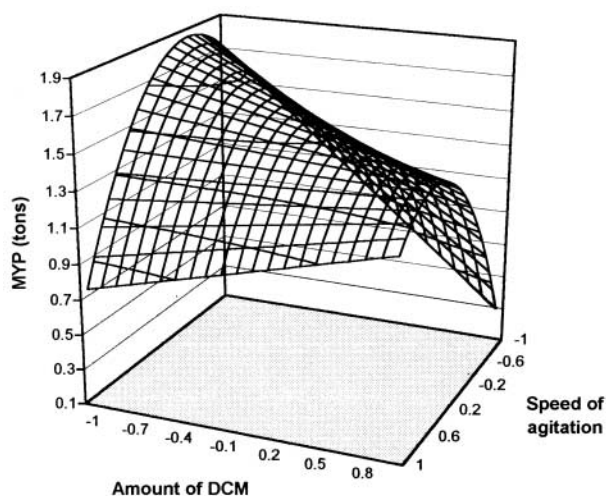


Figure 6. Effect of variables on mean yield pressure (MYP).

the agglomerates obtained exhibited the lowest MYP due to less dense agglomerates breaking at relatively low pressures to generate a greater area for particle-particle interaction.

#### Dissolution Study

Complete dissolution of drug from the compacts of agglomerates occurred within 45–60 min. As shown in Fig. 7, the drug dissolution profiles of compacted agglomerates are comparable with the marketed formulation. During dissolution studies it was observed that compacts disintegrated in 10–15 min to release the aggregated particles of the drug which did not break due to lack of intragranular disintegrant. The slower drug release from batch C4 may be attributed to the higher crushing strength of the agglomerates released after disintegration of the compact.

The amount of drug dissolved in 45 min ( $D_{45}$ ) was found to be significantly affected by both variables. The response surface (Fig. 8) shows that  $D_{45}$  is mainly a quadratic function of the variables. Initially, with increase in amount of DCM,  $D_{45}$  was found to decrease. In this region the less dense agglomerates formed, forming compacts which disintegrate to produce stronger aggregates of particles giving slower dissolution rates. In the latter region  $D_{45}$  values increased, which may be attributed to the predominating effect of loss of HPMC.

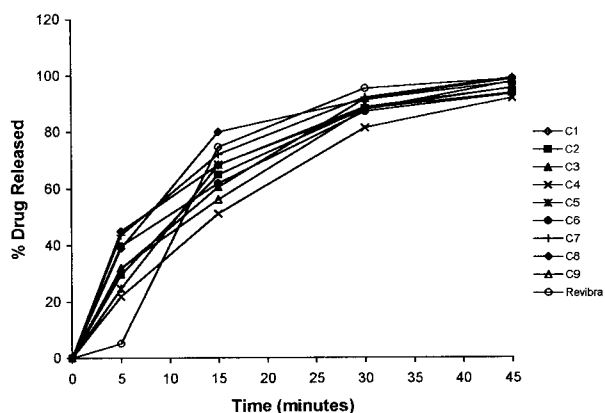


Figure 7. Dissolution profile of compacts of celecoxib agglomerates and marketed product.

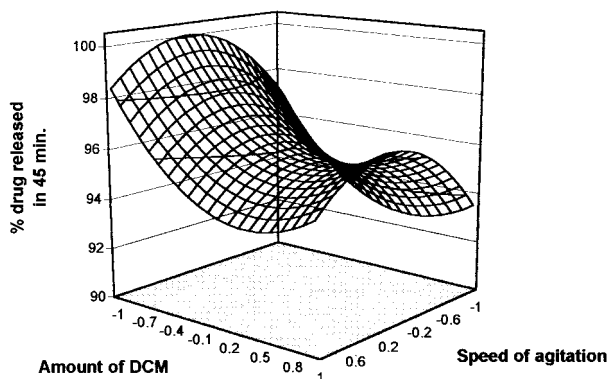


Figure 8. Effect of variables on per cent drug dissolved in 45 min ( $D_{45}$ ).

The  $D_{45}$  values increased initially with increase in speed of agitation and decreased thereafter. This may also be attributed to the relation between agglomerate compactness, HPMC content, and size of aggregates formed after disintegration, as discussed earlier.

#### CONCLUSIONS

Celecoxib agglomerates obtained by the solvent change method exhibited decreased drug crystallinity and satisfactory micromeritic, mechanical, and compressional properties. Response surface methodology was found to be a useful tool to study the effect of variables. The amount of bridging liquid and speed of agitation significantly affect the

micromeritic and compressional properties of the agglomerates. The compacts of the agglomerates have shown in vitro drug release performance comparable with the marketed capsule formulation. Therefore, this technique can be exploited to obtain agglomerates of celecoxib for tableting.

### ACKNOWLEDGMENTS

The authors are thankful to M/s Emcure Pharmaceuticals Ltd. for providing a gift sample of celecoxib. The authors A.R.P. and J.K.C. are grateful to the All India Council for Technical Education, New Delhi for providing a financial assistance in the form of a TAPTEC project grant and Junior Research Fellowship, respectively. A.R.K. and V.B.P. are thankful to the Council of Scientific and Industrial Research, New Delhi for support in the form of a Senior Research Fellowship.

### REFERENCES

1. Kawashima, Y.; Okumara, M.; Takenaka, H. *Science* **1982**, *216*, 1127–1128.
2. Kawashima, Y.; Okumara, M.; Takenaka, H.; Kojima, N. *J. Pharm. Sci.* **1984**, *73*, 1535–1538.
3. Kawashima, Y.; Okumara, M.; Takenaka, H. *Powder Technol.* **1984**, *39*, 41–47.
4. Pawar, P.H.; Pawar, A.P.; Mahadik, K.R.; Paradkar, A.R. *Indian J. Pharm. Sci.* **1998**, *60*(1), 24–28.
5. Deshpande, M.C.; Mahadik, K.R.; Pawar, A.P.; Paradkar, A.R. *Indian J. Pharm. Sci.* **1997**, *59*(1), 32–34.
6. Ueda, M.; Nakamura, Y.; Makita, H.; Imasato, Y.; Kawashima, Y. *Chem. Pharm. Bull.* **1990**, *38*, 2537–2541.
7. Sano, A.; Kuriki, T.; Kawashima, Y.; Takeuchi, H.; Hino, T.; Niwa, T. *Chem. Pharm. Bull.* **1990**, *38*, 733–738.
8. Sano, A.; Kuriki, T.; Kawashima, Y.; Takeuchi, H.; Hino, T.; Niwa, T. *Chem. Pharm. Bull.* **1992**, *40*, 1573–1576.
9. Sano, A.; Kuriki, T.; Kawashima, Y.; Takeuchi, H.; Hino, T.; Niwa, T. *Chem. Pharm. Bull.* **1992**, *40*, 3030–3035.
10. Sano, A.; Kuriki, T.; Handa, T.; Takeuchi, H.; Kawashima, Y. *J. Pharm. Sci.* **1987**, *76*, 471–474.
11. Kawashima, Y.; Niwa, T.; Takeuchi, H.; Hino, T.; Itoh, Y.; Furuyama, S. *J. Pharm. Sci.* **1991**, *80*, 472–476.
12. Ganderton, D.; Hunter, B.M. *J. Pharm. Pharmacol.* **1971**, *23*, 1s–10s.
13. Vela, M.T.; Fernandez, A.M.; Rabasco, A.M. *Drug Dev. Ind. Pharm.* **1990**, *16*, 295–300.
14. Jarosz, P.J.; Parrot, E.L. *J. Pharm. Sci.* **1993**, *72*(5), 530–535.
15. Rubinstein, M.H.; Musikabhum, P. *Pharma Acta Helv.* **1978**, *53*, 125–126.
16. Strickland Jr., W.A.; Busse, L.W.; Higuchi, T. *J. Am. Pharm. Assoc.* **1956**, *45*(7), 482–486.
17. Nocent, M.; Bertocchi, L.; Espitalier, F.; Baron, M.; Couarraze, G. *J. Pharm. Sci.* **2001**, *90*(10), 1620–1625.
18. Grulke, E.A. *Solubility Parameters Values*. In *Polymer Handbook*, 3rd Ed.; John Wiley & Sons: New York, 1976; 519.
19. Morishima, K.; Kawashima, Y.; Kawashima, Y.; Takeuchi, H.; Niwa, T.; Hino, T. *Powder Technol.* **1993**, *76*, 57–64.
20. Shirakura, O.; Yamada, M.; Hashimoto, M.; Ishimau, S.; Takayama, K.; Nagai, T. *Drug Dev. Ind. Pharm.* **1991**, *17*(4), 471–483.





Copyright of Drug Development & Industrial Pharmacy is the property of Taylor & Francis Ltd and its content may not be copied or emailed to multiple sites or posted to a listserv without the copyright holder's express written permission. However, users may print, download, or email articles for individual use.